DOI 10.1007/s11141-016-9722-6
Radiophysics and Quantum Electronics, Vol. 59, No. 7, December, 2016
(Russian Original Vol. 59, No. 7, July, 2016)

DETERMINATION OF THE TRACE-GAS CONCENTRATIONS AT THE ALTITUDES OF THE LOWER AND MIDDLE MESOSPHERE FROM THE TIME SERIES OF OZONE CONCENTRATION

A. A. Nechaev,* T. S. Ermakova, and M. Yu. Kulikov UDC 551.510

We present a statistical (Bayesian) approach to retrieving the concentrations of the most important mesospheric trace gases at altitudes of 50–75 *km using the photochemical model based on the time series of ozone concentration, which are measured during the daylight hours in one day with the help of the ground-based passive microwave devices. Using the model noisy time series of ozone concentration with allowance for the realistic accuracy of its measurements in the mesosphere, which is ensured by the available ozonometers, the accuracy of retrieving the nonmeasurable mesospheric characteristics is studied as a function of the altitude and the time-series length.*

1. INTRODUCTION

Since ozone is one of the most important atmospheric trace gases, the study of its spatiotemporal evolution is conventionally considered to be a basic problem in the terrestrial-atmosphere studies. First, the ozone layer, which is mainly located at the lower- and middle-stratosphere altitudes, protects all the planet living organisms from the ultraviolet solar radiation. Second, the photochemical processes relate evolution of the concentration of this component to that of the concentrations of other atmospheric trace gases. Third, the spatiotemporal distribution of the ozone concentration is measured (rather successfully) on the regular basis by various remote methods using the satellite-borne and ground-based equipment. The results of these measurements (e.g., in the form of the spatiotemporal series of the ozone concentration) allow one to retrieve the nonmeasurable or poorly measurable atmospheric characteristics with the help of the inverse-simulation methods and photochemical (transport-photochemical) models of the corresponding atmospheric region. This work is aimed at the development of such an approach to the problem of monitoring the key chemical mesospheric components from the Earth's surface.

The mesosphere is located in the altitude range 50–90 km between the above-located thermosphere, whose state is to a greater extent determined by variability of the solar-radiation characteristics, and the underlying stratosphere. This region substantially absorbs the most active portion of the solar radiation (in particular, the short-wavelength ultraviolet radiation is absorbed almost completely) and the high-intensity precipitation of the high-energy particles and, therefore, is in fact the second important (after the magnetosphere) layer protecting the human environment from the ruinous solar influence. On the other hand, since the mesosphere is an important component of the radiative transfer and transformation in the Sun–atmosphere–Earth's surface and ocean–atmosphere–cosmic space systems, evolution of parameters in this region influences the global atmospheric processes. In the upper part of the mesosphere (in a mesopause region of 80–90 km), the temperature reaches its minimum value about 100 K [1] in the Earth's

* ant.a.nech@gmail.com.

Institute of Applied Physics of the Russian Academy of Sciences, Nizhny Novgorod, Russia. Translated from Izvestiya Vysshikh Uchebnykh Zavedenii, Radiofizika, Vol. 59, No. 7, pp. 605–619, July 2016. Original article submitted June 22, 2015; accepted November 25, 2015.

atmosphere, which makes this region very thermally sensitive. For these reasons, the characteristics of the mesospheric physicochemical processes are important indicators of the possible variations in the entire-atmosphere state due to both variations in the natural factors and artificial effects and are studied by many research collaborations (e.g., Network for the Detection of Mesospheric Change [2]).

The components of the families of odd oxygen compounds O_x (O, $O(^1D)$, and O_3) and odd hydrogen compounds HO_x (H, OH, and HO_2) [3] are among the most important mesospheric trace gases (TGs), which, in particular, determine the photochemical mesospheric-air heating caused by exothermal reactions. In turn, the local evolution of the above-mentioned compounds is mainly determined by the diurnal illuminance variations leading to the corresponding modulation of the photodissociation coefficients and the parameter values among which the water-vapor concentration is the most variable (in both space and time). Experimental observation of the above-mentioned components is performed from aircraft, stratospheric balloons, rockets, satellites, and Earth's surface [4–11]. However, for some reasons (mainly because of the high cost), the air-borne, stratospheric-balloon, and rocket-borne measurements are occasional. Therefore, exhaustive studies are performed in the course of special short-term campaigns and expeditions and the results of such campaigns allow one to reveal the detailed mechanisms of the observed phenomena. Only a small number of the above-mentioned components are measured on the regular basis (ozone and hydroxyl from the satellites and only ozone from the Earth's surface).

In [12, 13], the method for retrieving the vertical distributions of the concentrations of atomic oxygen and hydrogen, hydrogen peroxide, and water vapors at altitudes of 50–87 km from the daytime simultaneous satellite measurements of the ozone and hydroxyl concentrations is developed using the model of the mesospheric photochemical system (MPCS). Its efficiency was demonstrated by an example of the CRISTA–MAHRSI experimental data. It is shown that at least two pairs of vertical distributions of the O_3- and OH-component concentrations, which are measured during the daylight period in the morning and afternoon hours of one day at the points with close horizontal coordinates, should be available for implementing this method. By virtue of its features, the satellite-borne atmospheric scanning allows one to use such an approach only for individual spatial points and rather irregularly even at these points. As distinct from the satellite observations, the atmospheric microwave passive sensing from the Earth's surface in the corresponding atmospheric transparency windows allows one to perform the measurements almost at any spatial point with the chosen horizontal coordinates and accumulate long time series of the vertical ozone-concentration profiles at the mesospheric altitudes, including those during each daylight period. At present, about ten ozonometers are almost continuously used by the international organization NDACC (the former NDSC) [14]. In Russia, regular ozonometric observations are also conducted in Moscow, St. Petersburg, and Nizhny Novgorod (see, e.g., [15–18]) using both the stationary devices and their mobile variants.

The method of microwave ozone sensing from the Earth's surface is based on the observations of the integral line of natural atmospheric radiation, which is formed by one of the resonance lines of the ozone molecule having rotational spectra in the millimeter and submillimeter wave ranges. Compared with the measurements in the optical and infrared wavelength ranges, which are performed using lidars, the microwave measurements are less dependent on the weather conditions and the aerosol atmospheric component and can be performed round the clock. It should also be noted that retrieval of the vertical profile of ozone concentration from the data of radiometric sensing from the Earth's surface is an inverse ill-posed problem. Accuracy of retrieval of the concentration distribution of this trace gas is mainly determined by the equipment sensitivity and the time of accumulation of the corresponding experimental spectra. Moreover, at the mesospheric altitudes, the absolute ozone concentration decreases with increasing altitude, which inevitably deteriorates the accuracy of the ozone-concentration measurements by the microwave methods and should finally result in an increase in the uncertainty of retrieval of other mesospheric characteristics from these data using the photochemical model.

In this work, we present the statistical (Bayesian) approach to retrieving the concentrations of the most important mesospheric trace gases at altitudes of 50–75 km from the time series of ozone concentration, which are measured during one daylight period using the microwave passive ground-based equipment. The

quality of retrieving the nonmeasurable mesospheric characteristics (the concentrations of atomic oxygen and hydrogen, hydroxyl, hydrogen peroxide, and the water vapors) as functions of the altitude and the time-series length is studied using the model noisy time series of the concentration of the ozone component with allowance for the realistic accuracy of its measurements in the mesosphere by the well-known ozonometers. It is shown that using *a priori* information on the distribution of the water-vapor (H_2O) concentration, one can significantly improve the ozone-concentration retrieval accuracy over the entire altitude range, decreasing the displacement of its mean profile with respect to the "true" one (i.e., specified in the model).

Our work is organized as follows. Section 2 describes the general approach to retrieving the unknown characteristics of the dynamic model. Section 3 represents the mesospheric photochemical system and the used model of this system. The basic results of retrieving the concentrations of the mesospheric trace gases are given in Sec. 4. The further directions of development of the proposed method and its applications to the actual observation data are discussed in Sec. 5.

2. STATISTICAL APPROACH TO RETRIEVING THE UNKNOWN CHARACTERISTICS OF THE DYNAMIC MODEL

The proposed approach to retrieving the nonmeasurable mesospheric trace gases from the time series of ozone concentration is based on the method described in [19].

Let us have a system of N differential equations whose right-hand sides depend on one unknown parameter μ:

$$\frac{\mathrm{d}\mathbf{u}}{\mathrm{d}t} = \mathbf{f}(t, \mathbf{u}, \mu), \qquad \mathbf{u} \in R^N. \tag{1}$$

, Let the time series $X\{x_m^{(0)}, x_m^{(1)}, \ldots, x_m^{(L-1)}\}$ obtained during the observation experiment consist of L sequential values of the mth ($1 \le m \le N$) dynamic variable to which the following random measurement error specified by the probability density $w(\xi^{(0)}, \xi^{(1)}, \ldots, \ldots, \xi^{(L-1)})$ is added:

$$x_m^{(i)} = u_m^{(i)} + \xi^{(i)}, \qquad u_m^{(i)} = u_m(t = t_i), \qquad i = 0, 1, \ldots L-1 \tag{2}$$

. Using the series X, one should retrieve the unknown value of the parameter μ and the time evolutions $\mathbf{u}^{(i)} = \mathbf{u}(t = t_i)$, where $i = 0, 1, \ldots L-1$, of all latent (noise-hidden) variables.

We note that this problem is mathematically ill-posed, i.e., the small errors in the initial data can lead to substantial errors in the values of the retrieved characteristics. Using the Bayesian method for solving inverse problems, which allows for the statistic of the random measurement component, is one of the approaches to overcoming this difficulty. The main idea is to develop the probability density $P(\mu \mid X)$ of the unknown parameter under the condition that the particular time series X is observed. The moments of this distribution allow us to determine the values of the unknown parameter from the noisy data with specified probability. The values of the dynamic variables at various times are interrelated via the mapping of the flow generated by differential equation (1):

$$\mathbf{u}^{(i)} = \mathbf{G}(t_i, \mathbf{u}^{(0)}, \mu) \qquad i = 0, 1, \ldots L-1. \tag{3}$$

This allows us to write a simple expression for the conditional distribution density of the latent variables as

$$P(\mathbf{u}^{(1)}, \ldots, \mathbf{u}^{(L-1)} \mid \mathbf{u}^{(0)}, \mu) = \prod_{i=1}^{L-1} \delta[\mathbf{u}^{(i)} - \mathbf{G}(t_i, \mathbf{u}^{(0)}, \mu)]. \tag{4}$$

in which $\delta(y)$ is a Dirac function.

We assume that the noise components are mutually independent at different times, which is quite

natural for ozonometric observations, i.e.,

$$w(\xi^{(0)}, \xi^{(1)}, \ldots, \xi^{(L-1)}) = \prod_{i=0}^{L-1} w(\xi^{(i)}), \tag{5}$$

and find the distribution density of the probabilities of observing the series X if the latent-variable values and the parameter μ are specified:

$$P(X \mid \mathbf{u}^{(0)}, \ldots, \mathbf{u}^{(L-1)}, \mu) = \prod_{i=0}^{L-1} w^{(i)}(x_m^{(i)} - u_m^{(i)}). \tag{6}$$

Performing convolution of the two probability densities, with allowance for the identity $\mathbf{G}(t_0, \ldots) \equiv \mathbf{u}^{(0)}$, we obtain the likelihood function of the model:

$$P(X \mid \mathbf{u}^{(0)}, \mu) = \iint \ldots \int P(X \mid \mathbf{u}^{(0)}, \ldots, \mathbf{u}^{(L-1)}, \mu) P(\mathbf{u}^{(1)}, \ldots, \mathbf{u}^{(L-1)} \mid \mathbf{u}^{(0)}, \mu)\, \mathrm{d}\mathbf{u}^{(1)} \ldots \mathrm{d}\mathbf{u}^{(L-1)}$$
$$= \prod_{i=1}^{L-1} w^{(i)}[x_m^{(i)} - G_m(t_i, \mathbf{u}^{(0)}, \mu)]. \tag{7}$$

Using the Bayes theorem, with accuracy up to the normalization coefficient, we write the expression for the *a posteriori* probability density of the nonobserved quantities $\mathbf{u}^{(0)}$ and μ:

$$P(\mathbf{u}^{(0)}, \mu \mid X) \propto P(X \mid \mathbf{u}^{(0)}, \mu) P(\mathbf{u}^{(0)}, \mu) = P(\mathbf{u}^{(0)}, \mu) \prod_{i=0}^{L-1} w^{(i)}[x_m^{(i)} - G_m(t_i, \mathbf{u}^{(0)}, \mu)], \tag{8}$$

in which the probability density $P(\mathbf{u}^{(0)}, \mu)$ represents *a priori* assumptions on the possible values of the unknown characteristics. They can be based on the statistics of their long-term measurements for a particular time and place or result from the "physical" restrictions imposed on definition domain (8), e.g., reflect the fact that the chemical-component concentrations cannot be negative. It is shown in Sec. 4 that in the case considered, using the informative *a priori* function $P(\mathbf{u}^{(0)}, \mu)$, which results in localization of distribution (8), we can substantially improve the retrieval accuracy of the parameter-μ.

The desired probability density $P(\mu \mid X)$ of the unknown parameter is obtained by the N-tuple integration of Eq. (8) with respect to the latent variables at the initial time instant:

$$P(\mu \mid X) = \iint \ldots \int P(\mathbf{u}^{(0)}, \mu \mid X)\, \mathrm{d}\mathbf{u}^{(0)}. \tag{9}$$

The probability distribution of the jth latent variable at the ith time instant is determined by the expressions

$$P(\mathbf{u}^{(i)}, \mu \mid X) = P[\mathbf{G}^{-1}(t_i, \mathbf{u}^{(i)}, \mu), \mu \mid X]\, |J_G(\mathbf{u}^{(i)}, \mu)|^{-1}, \tag{10}$$

$$P(\mathbf{u}_j^{(i)} \mid X) = \iint \ldots \int P(\mathbf{u}^{(i)}, \mu \mid X)\, \mathrm{d}\mathbf{u}_1^{(i)} \ldots \mathrm{d}\mathbf{u}_{j-1}^{(i)}\, \mathrm{d}\mathbf{u}_{j+1}^{(i)} \ldots \mathrm{d}\mathbf{u}_N^{(i)}\, \mathrm{d}\mu, \tag{11}$$

where $J_G(\mathbf{u}^{(i)}, \mu)$ is the Jacobian of transform (3).

3. MESOSPHERIC PHOTOCHEMICAL SYSTEM

The mesospheric photochemical system (MPCS) describes the most important photochemical processes observed at altitudes of 50–90 km. It usually includes 20 of the most significant reactions with

participation of the components belonging to the family of odd compounds of oxygen O_x (O, $O(^1D)$, O_3) and hydrogen HO_x (H, OH, HO_2), whose concentrations vary with a characteristic time scale of 10^4–10^5 s at the altitudes of the lower and middle mesospheres:

1) $O + OH + M \to HO_2 + M$, 2) $H + HO_2 \to O_2 + H_2$, 3) $OH + HO_2 \to O_2 + H_2O$,
4) $O + OH \to O_2 + H$, 5) $O + HO_2 \to O_2 + OH$, 6) $O_2 + H + M \to HO_2 + M$,
7) $H_2O + h\nu \to H + OH$, 8) $O_2 + h\nu \to 2O$, 9) $O + O_2 + M \to O_3 + M$,
10) $O + O_3 \to 2O_2$, 11) $O + O + M \to O_2 + M$, 12) $O_3 + H \to O_2 + OH$,
13) $O_3 + OH \to O_2 + HO_2$, 14) $H + HO_2 \to 2OH$, 15) $OH + OH \to O + H_2O$,
16) $O_3 + h\nu \to O_2 + O$, 17) $OH + H + M \to H_2O + M$, 18) $H + HO_2 \to O + H_2O$,
19) $O(^1D) + M \to O + M$, 20) $H_2O + O(^1D) \to 2OH$.

This system is subject to external action with a period of 24 h, which is related to the Earth rotation and manifested in periodic modulation of the coefficients of photodissociation of the ozone molecules, water vapor, and molecular oxygen (reactions 16, 7, and 8, respectively). The temperature T, on which the rates of the majority of the above-mentioned reactions depend, the concentrations of the air molecules M and water vapor, and the zenith angle of the Sun and the altitude, on which the above-mentioned photolysis processes depend, are the key parameters.

It is well known that under the actual mesospheric conditions, evolution of the trace-gas concentrations can be strongly influenced by the transfer processes (molecular and turbulent diffusion, horizontal and vertical winds, and planetary and internal gravity waves). In what follows, we confine ourselves to considering the altitude range 50–75 km in which the "individual" characteristic times of each of the above-mentioned transfer processes exceed (by more than an order of magnitude) the MPCS-evolution time scale and, therefore, the zero-dimensional model of this system can be used. In addition, since the component $O(^1D)$ has a very short lifetime in the mesosphere (about 10^{-3}–10^{-6} s), this component can be excluded from the dynamic variables and its concentration can be determined from the condition of instantaneous stable equilibrium.

The coefficients of reactions 16, 7, and 8 for the particular values of latitude, longitude, and the number of the day of the year are calculated using the corresponding models of the ultraviolet solar-radiation transfer through the atmosphere, and the distributions $T(z)$ and $M(z)$ at the mesospheric altitudes are effectively measured by the satellite-borne sensing equipment and satisfactorily retrieved by the modern meteorological middle-atmosphere models. In this work, the profiles $T(z)$ and $M(z)$, which correspond to the mid-August and the latitude range 55–60° N, are used for definiteness and the dependences of the photodissociation coefficients on the altitude and local time (see Fig. 1) are calculated within the framework of the COMMA–IAP model [20].

Therefore, the initial MPCS model is a system of five differential equations of the first order with respect to time for the concentrations of the components O, O_3, H, OH, and HO_2. If $T(z)$, $M(z)$, and the dependences of the photodissociation coefficients on the altitude and the time of the day, are fixed, then the dynamics of the model is determined by the distribution of only one parameter, namely, the water-vapor concentration whose spatiotemporal variability is much greater than that of the air temperature and concentration. Thus, in what follows, to solve the direct problem, we use the altitude profile of the water-vapor concentration, which was obtained by averaging the MLS Aura satellite sounding data obtained on August 14–15 for an latitude range of 55–60° N. The ozone-concentration time series, which were calculated within the framework of the MPCS model, were further exposed to noise and used for solving the inverse problem according to the approach presented in Sec. 2 and then the results of retrieval of the MPCS parameter and dynamic variables were compared with their true values. The retrieval quality of these characteristics is obviously a function of altitude, the length of the initial time series of the ozone concentration, and the value of its measurement noise. In this work, the characteristics of the "noise" probability density correspond to those of two well-known ozonometers OZORAM [21] and GROMOS [22], and noise is assumed to

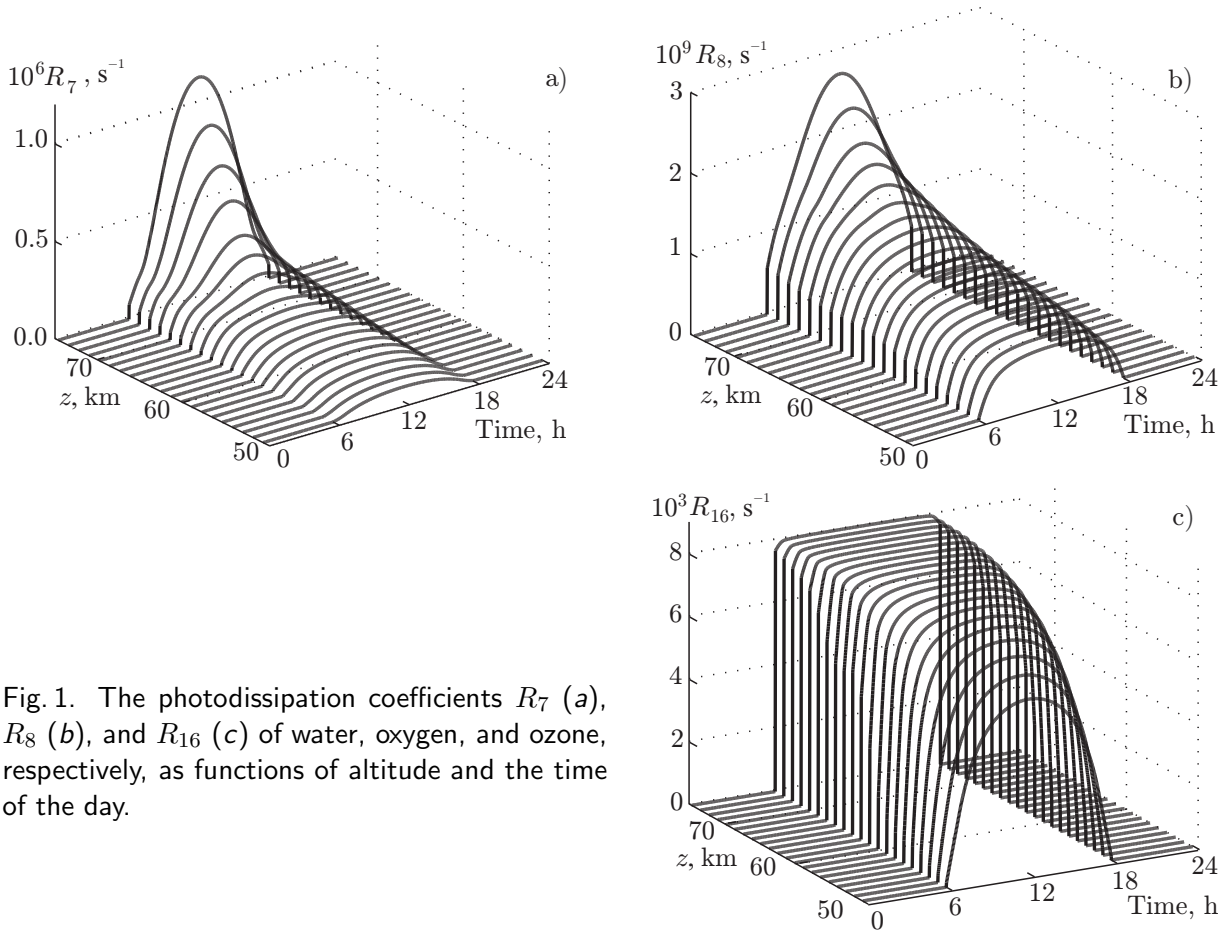

Fig. 1. The photodissipation coefficients R_7 (*a*), R_8 (*b*), and R_{16} (*c*) of water, oxygen, and ozone, respectively, as functions of altitude and the time of the day.

be Gaussian with the altitude-dependent variance:

$$w^{(i)}(\xi^{(i)}) \propto \exp\left\{-\frac{1}{2}\left[\frac{\xi^{(i)}}{\sigma^{(i)}_{\mathrm{O_3}}(z)}\right]^2\right\}. \tag{12}$$

It should be noted that since the differential equations of the MPCS model are nonlinear, it is analytically impossible to find the functions $\mathbf{G}(\dots)$ of mapping (3) and integrate the *a posteriori* probability density $P(\mathrm{O}^{(0)}, \mathrm{O}_3^{(0)}, \mathrm{H}^{(0)}, \mathrm{OH}^{(0)}, \mathrm{HO}_2^{(0)}, \mathrm{H_2O}|X)$ of the latent variables and the parameter (X is the initial time series of the ozone concentration). Hereinafter, O_x, H, OH, HO_x, and $\mathrm{H_2O}$ are the concentrations of the corresponding components. To numerically integrate this function, it is expedient to use the Monte Carlo method based on the Metropolis–Hastings algorithm [23]. It allows one to effectively generate an exhaustive set of the observed quantities of $\mathrm{O}^{(0)}$, $\mathrm{O}_3^{(0)}$, $\mathrm{H}^{(0)}$, $\mathrm{OH}^{(0)}$, $\mathrm{HO}_2^{(0)}$, and $\mathrm{H_2O}$, which comprises about ten thousand combinations of their values and is distributed with normalized density (8). Equating to zero the coordinates of the points of the six-dimensional space, which correspond to the values of the latent variables, i.e., projecting the constructed set onto the one-dimensional subspace, we obtain an ensemble distributed with the objective density $P(\mathrm{H_2O}|X)$. The statistical moments of this function are obtained by summing over the ensemble elements. It should also be noted that in this case, the probability density $P(u_j^{(i)}|X)$ of the jth latent variable at the ith time instant is directly determined in the process of calculating $P(\mathrm{O}^{(0)}, \mathrm{O}_3^{(0)}, \mathrm{H}^{(0)}, \mathrm{OH}^{(0)}, \mathrm{HO}_2^{(0)}, \mathrm{H_2O}|X)$ by constructing the histogram of the values of the function $G_j(t_j, \mathrm{O}^{(0)}, \mathrm{O}_3^{(0)}, \mathrm{H}^{(0)}, \mathrm{OH}^{(0)}, \mathrm{HO}_2^{(0)}, \mathrm{H_2O}|X)$ on the ensemble of nonobservable quantities, which is generated by the Metropolis–Hastings algorithm.

4. THE RESULTS OF RETRIEVING THE MESOSPHERIC TRACE GASES

During the study, the above-described approach was used for various altitudes z and the time-series lengths L without *a priori* information and with addition of the informative *a priori* part

$$P(\mathbf{u}^{(0)}, \mathrm{H_2O}) \propto \exp\left\{-\frac{1}{2}\left[\frac{\mathrm{H_2O} - \langle \mathrm{H_2O}\rangle_{\mathrm{apr}}(z)}{\sigma_{\mathrm{apr}}(z)}\right]^2\right\} \tag{13}$$

to *a posteriori* function (8). Here, the mean profile $\langle \mathrm{H_2O}\rangle_{\mathrm{apr}}(z)$ and the variance $\sigma^2_{\mathrm{apr}}(z)$ are obtained by averaging the water-vapor concentration profiles measured by the MLS Aura in the daytime in the period August 1–31 of 2009–2014 in the latitude range 55–65° N.

In the first case, when choosing $P(\mathbf{u}^{(0)}, \mu)$, only the natural requirement of nonnegativeness of the trace-gas concentrations was allowed for:

$$P(\mathbf{u}^{(0)}, \mu) = \begin{cases} 1, & \text{for any } j\ \{\mathbf{u}^{(0)}, \mu\} \geq 0; \\ 0, & \text{in the opposite case.} \end{cases} \tag{14}$$

The probability density $P(\mathrm{H_2O} \mid X)$ of the water-vapor concentration, which was calculated using condition (14), is unimodal for all the altitude values. For the comparatively small lengths of the initial time series of ozone concentration, e.g., $L = 3$ (see Fig. 2*a*), it is close to the logarithmically normal distribution, which tends to transform to the normal one with increasing L (see Fig. 2*b*). Therefore, in the forthcoming analysis, we confine ourselves to considering two moments of these distributions, namely, the median $\langle \mathrm{H_2O}\rangle_{\mathrm{med}}$ and the variance $\sigma^2_{\mathrm{H_2O}}$.

Figures 3*a* and 3*b* show the results of retrieval of the water-vapor concentration from the model noisy series of the ozone-concentration measurements with the length $L = 11$, which correspond to the local times 8, 9,.., and 18 h. The measurement-noise values correspond to the accuracy of the ozone concentration measurements by the OZORAM and GROMOS devices with the time 1 h of accumulation and averaging of the microwave spectra of the natural atmospheric radiation. It can be seen that in an altitude range of about 60 to 70 km (up to 75 km for GROMOS), the relative variance $\sigma_{\mathrm{H_2O}}/\mathrm{H_2O}$ turns out to be smaller than the uncertainties σ_{OZORAM} and σ_{GROMOS} of the initial time series. At the same time, at some altitudes (e.g., 50–55 km and 70 km for GROMOS), displacement of the median $\langle \mathrm{H_2O}\rangle_{\mathrm{med}}$ with respect to the true value of $\mathrm{H_2O}$ is greater than the standard deviation $\sigma_{\mathrm{H_2O}}$. As is obvious from the repeated calculations, the location of the distribution median and, therefore, the displacement value strongly depend on the particular used noisy profile of ozone concentration, whereas $\sigma_{\mathrm{H_2O}}$ remains almost unchanged at altitudes of up to 75 km. At an altitude of 75 km, the repeated initiations of the algorithm with the OZORAM parameters ($\sigma_{\mathrm{OZORAM}}(75\ km) \approx 41\%$) yield the results which differ from one another by up to 10% for the same input profile $\mathrm{O_3}(z)$. This circumstance cannot be eliminated by varying the Metropolis-algorithm parameters.

Incorporating the *a priori* information to the *a posteriori* function, we improve the situation. The distribution localization using Eq. (13) allows one to obtain the reproducible retrieval result even for a very high uncertainty of the input data at a reasonable number of the generated-ensemble points. The relative retrieval error at all altitudes is significantly decreased (see Figs. 3*c* and 3*d*). The median-distribution displacement also turns out to be smaller than in the previous case when retrieving from the above-mentioned measurement series. Despite the fact that the mean distribution characteristics can still considerably vary if the input ozone-concentration profile is changed the displacement is not frequently observed.

In what follows, for brevity, we dwell on a more detailed analysis of the results of retrieving the nonmeasurable characteristics of the mesospheric photochemical processes as applied to the first ozonometer. Figure 4 shows the accuracy of the water-vapor concentration retrieval for various altitudes as a function of the length of the initial time series of ozone concentration for fixed value of the entire considered time range from 8 to 18 h. It can be seen that almost in all cases except for $L = 9$ and $L = 11$ at altitudes of

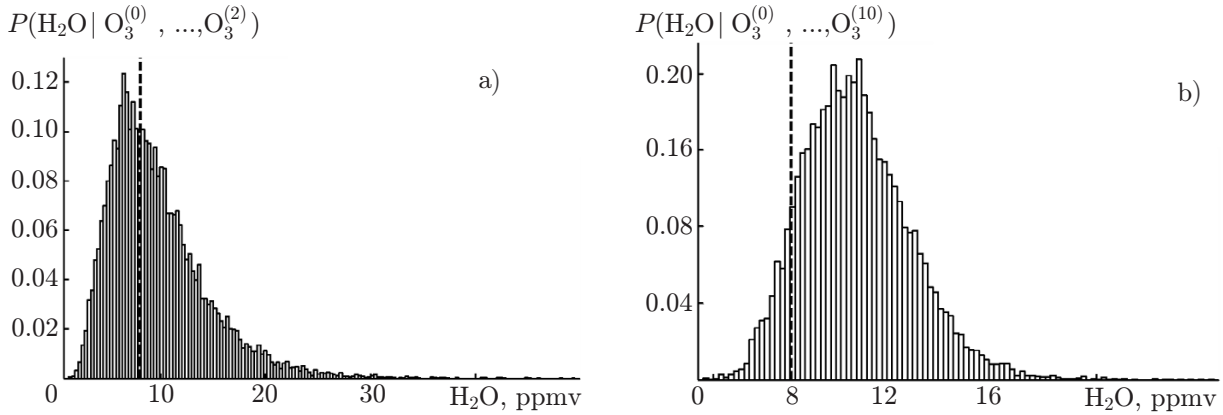

Fig. 2. The probability density of the water-vapor concentration for $z = 50$ km, retrieved from several ozone-concentration values with a noise variance of 11%. The dotted line shows the "true" value of the parameter $H_2O = 8.04$ ppmv, which was used during the calculation. On panel *a*, $L = 3$, the corresponding time moments are 8, 13, and 18 h, $H_2O = 8.04$ ppmv, and $\sigma_{H_2O} = 4.73$ ppmv. On panel *b*, $L = 11$, the time moments are 8, 9,.., 18 h, $\langle H_2O \rangle = 10.41$, and $\sigma_{H_2O} = 2.13$ ppmv.

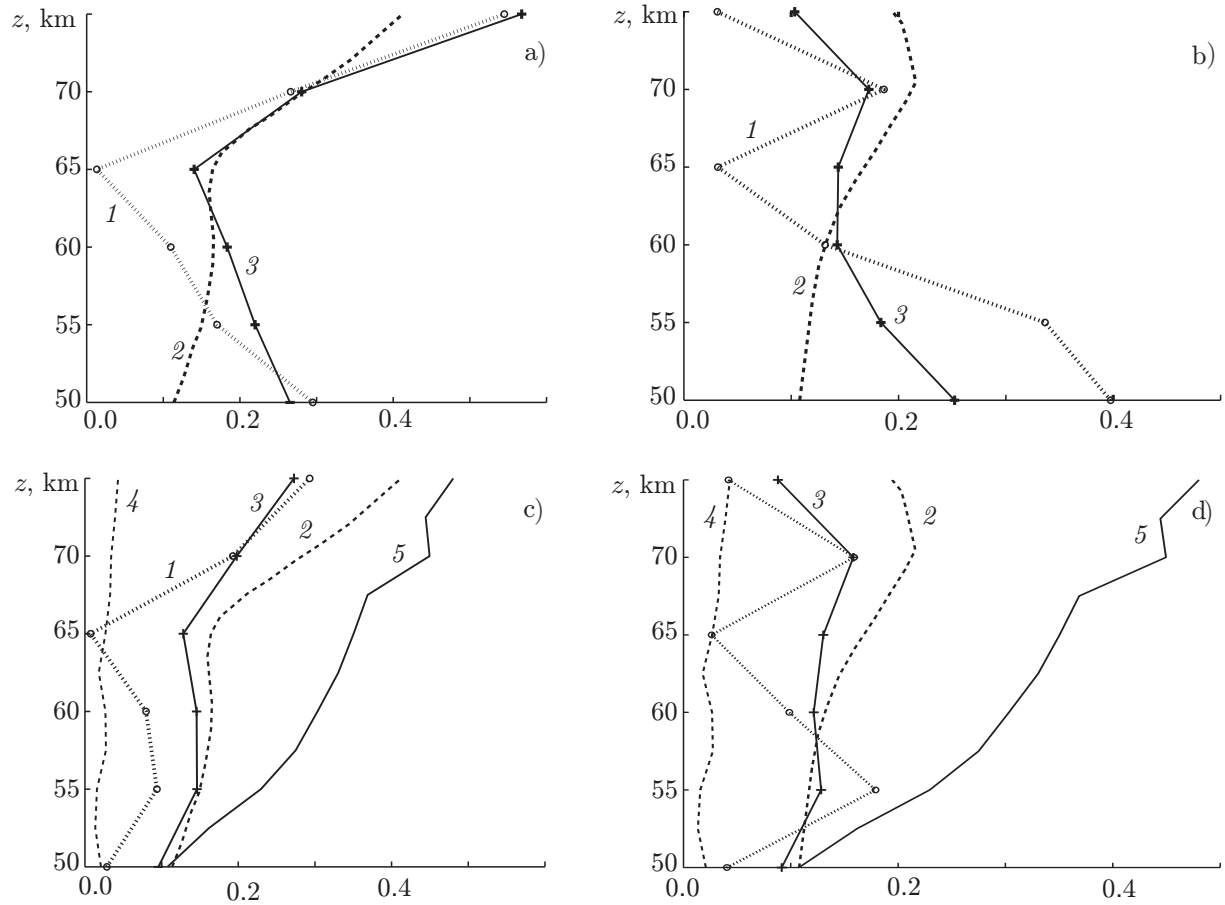

Fig. 3. Statistical moments of the water-vapor concentration distribution retrieved from the noisy ozone-concentration time series with the length $L = 11$. The noise values correspond to the accuracies of the ozone-concentration measurements by the devices OZORAM (*a* and *c*) and GROMOS (*b*, *d*). On panels *c* and *d*, the distributions are obtained using the informative *a priori* function. Curves *1* correspond to $|\langle H_2O \rangle_{med} - H_2O|/H_2O$, *2* to σ_{O_3}/H_2O, *3* to σ_{H_2O}/H_2O, *4* to $|\langle H_2O \rangle_{apr} - H_2O|/H_2O$, and *5* to σ_{apr}/H_2O.

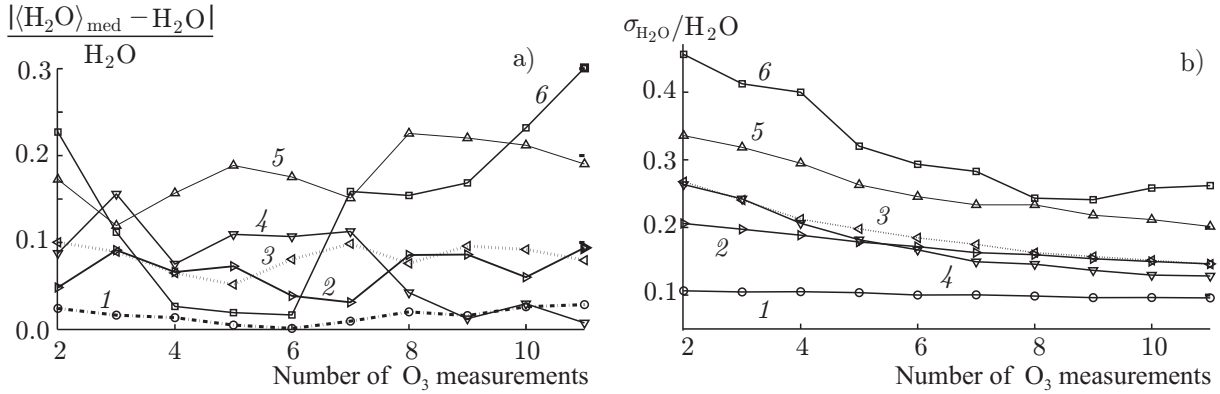

Fig. 4. Characteristics of the variance and median of the obtained probability densities of the water-vapor concentration at various altitudes as functions of the length of the initial time series of ozone concentration. Curves *1*, *2*, *3*, *4*, *5*, and *6* correspond to altitudes of 50, 55, 60, 65, 70, and 75 km, respectively.

60 and 75 km, respectively, the "true" value of the water-vapor (H_2O) concentration is located inside the boundaries $\langle H_2O\rangle_{med} \pm \sigma_{H_2O}$. As it should be expected, an increase in the series length leads to a decrease in the relative uncertainty σ_{H_2O}/H_2O.

Figures 5–9 show the results of retrieving the time evolution of the main dynamic variables of the MPCS for the initial-data time series length equal to 11. It is seen that, first, in an altitude range of 50–70 km, the method adequately (both qualitatively and quantitatively) allows one to determine the local concentrations of these components and, second, the accuracy of retrieving these mesospheric characteristics, including the ozone concentration, is on the average much better (severalfold or greater) than the measurement noise of the initial time series. In particular, the relative uncertainty $\sigma/\langle H\rangle$ at the altitudes above 65 km can reach 1%. Obviously, such a very high quality of retrieving the MPCS dynamic variables results from the fact that the used photochemical model effectively filters the initial noisy data on the ozone concentration. Thus, the relative uncertainty $\sigma/\langle O_3\rangle$ at the lower-mesospheric altitudes varies from 2% to 5% despite the fact that the initial data of this component were subject to noise with a variance of 11–16%.

Above 70 km, the retrieval quality is gradually deteriorated and in the first half of the daylight period at an altitude of 75 km, the local values of the dynamic variables of the MPCS can significantly differ from their true values, which fall outside the interval 2σ in the neighborhood of the mean value. It can be seen that for such levels of the initial-data noise, the retrieval results can be considered reliable only after local noon.

5. DISCUSSION AND CONCLUSIONS

In this work, we have proposed the method for retrieving the spatiotemporal evolution of the trace-gas concentrations in the lower and middle mesosphere from the noisy time series of the ozone concentration, which are measured by the ground-based ozonometric devices using the photochemical model of this atmospheric region. The results shown in Figs. 2–9 allow one to draw conclusions on the method capabilities in the case of using the actual observation data. First, as was shown in the model examples, the water-vapor concentration retrieval accuracy calculated on the basis of characteristics of the typical ozonometric devices with the use of *a priori* information amounts (in the case of long time series of the ozone-concentration measurements) to about 1–30%, depending on the altitude, which is in fair agreement with the errors of direct measurements of this component (e.g., by the ground-based microwave devices, which measure the natural atmospheric radiation in the water-vapor lines 22 and 183 GHz [14]). It should be noted that simultaneous microwave measurements of the vertical concentration profiles of the mesospheric components O_3 and H_2O are performed at the stations of the international NDACC network [14]. Using these data, we will be able to experimentally check the proposed-method accuracy by comparing the retrieved values of the

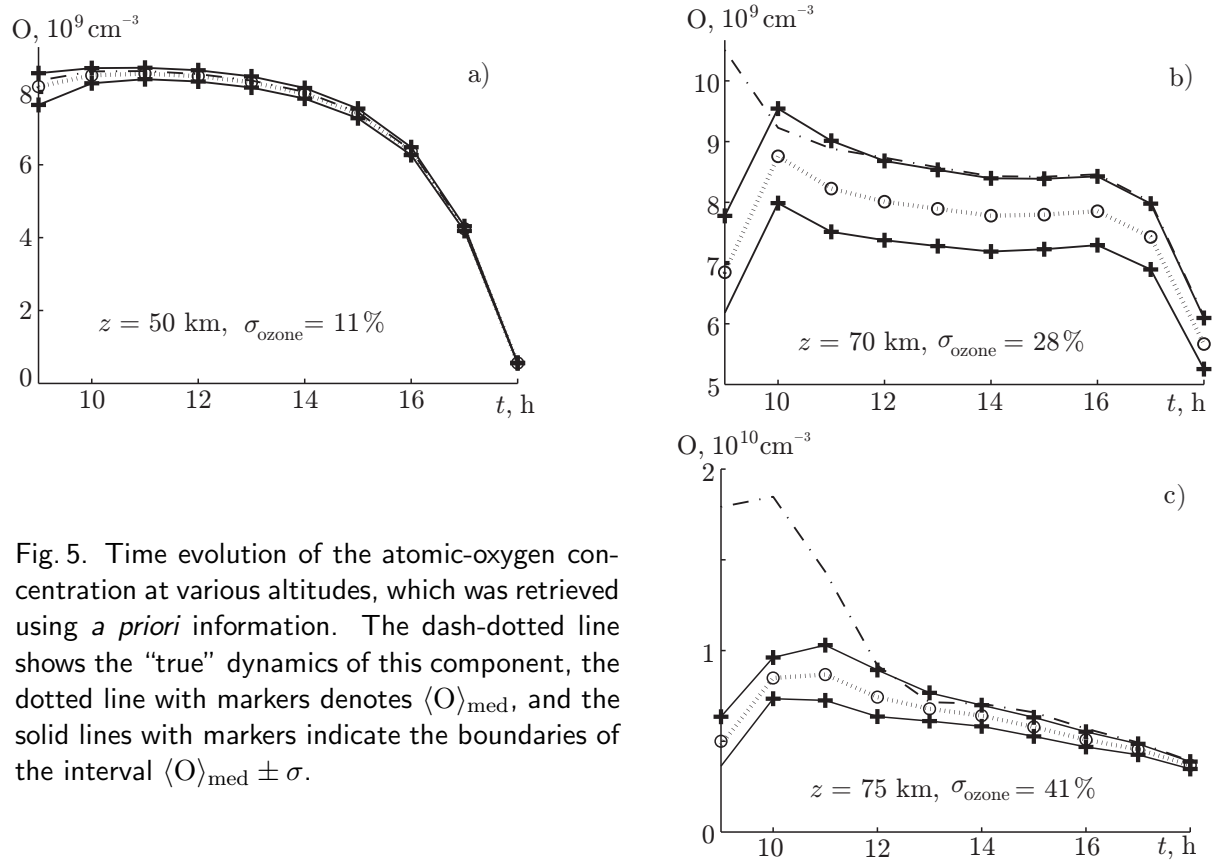

Fig. 5. Time evolution of the atomic-oxygen concentration at various altitudes, which was retrieved using *a priori* information. The dash-dotted line shows the "true" dynamics of this component, the dotted line with markers denotes $\langle \mathrm{O} \rangle_{\mathrm{med}}$, and the solid lines with markers indicate the boundaries of the interval $\langle \mathrm{O} \rangle_{\mathrm{med}} \pm \sigma$.

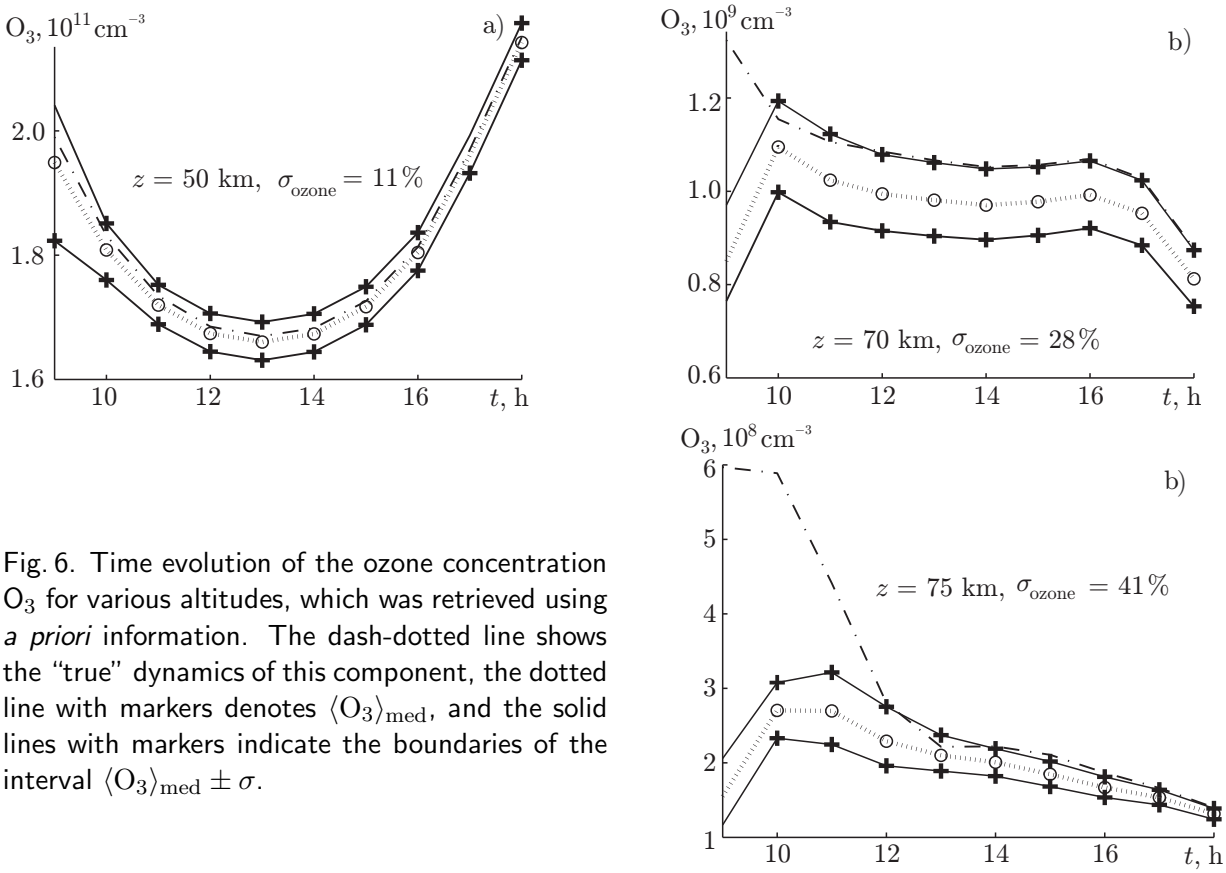

Fig. 6. Time evolution of the ozone concentration O_3 for various altitudes, which was retrieved using *a priori* information. The dash-dotted line shows the "true" dynamics of this component, the dotted line with markers denotes $\langle \mathrm{O}_3 \rangle_{\mathrm{med}}$, and the solid lines with markers indicate the boundaries of the interval $\langle \mathrm{O}_3 \rangle_{\mathrm{med}} \pm \sigma$.

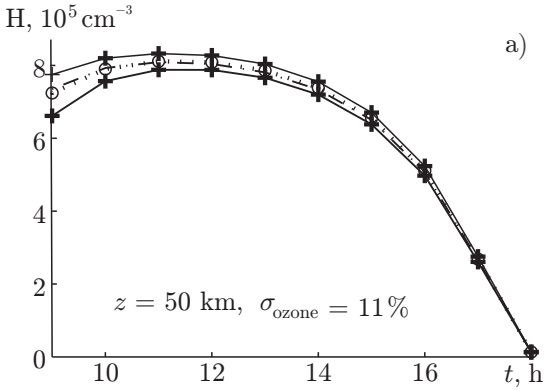

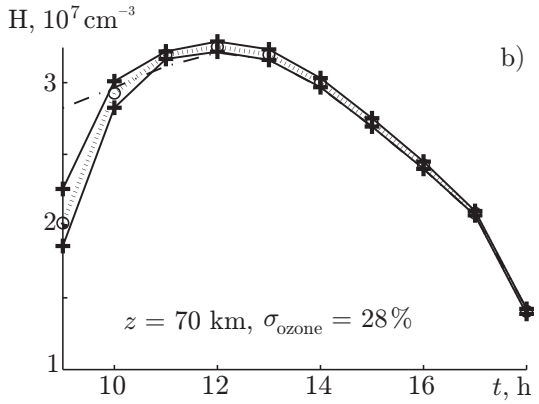

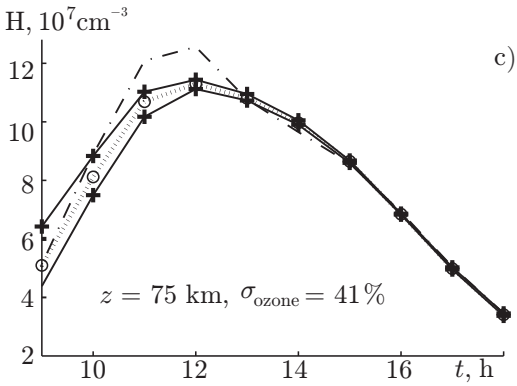

Fig. 7. Time evolution of the atomic-hydrogen concentration at various altitudes, which was retrieved using *a priori* information. The dash-dotted line shows the "true" dynamics of this component, the dotted line with markers denotes $\langle \mathrm{H} \rangle_{\mathrm{med}}$, and the solid lines with markers indicate the boundaries of the interval $\langle \mathrm{H} \rangle_{\mathrm{med}} \pm \sigma$.

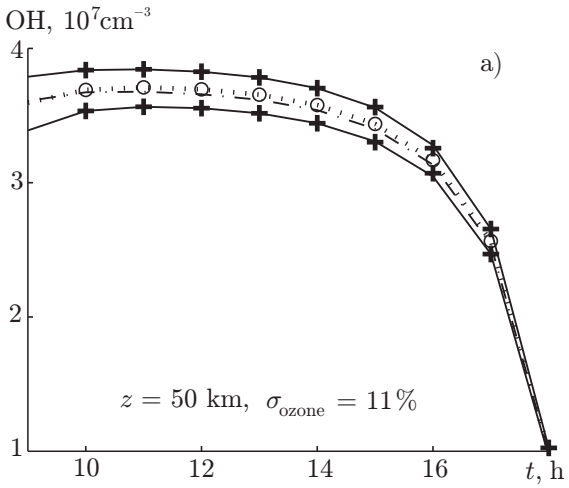

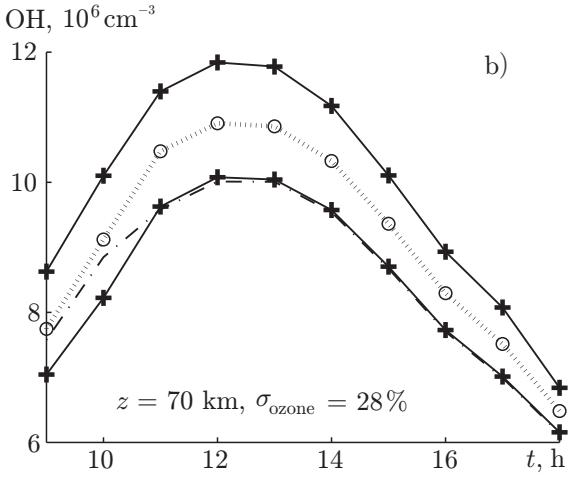

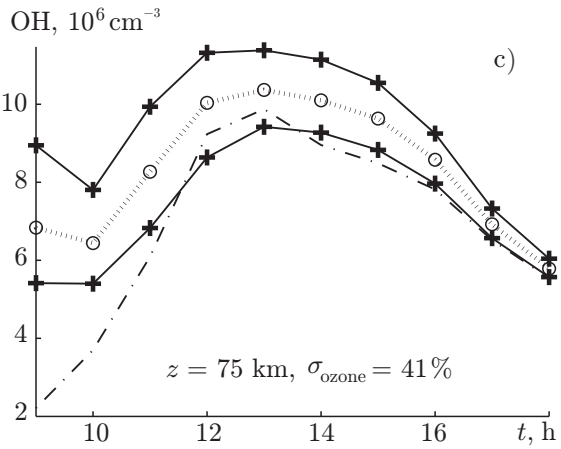

Fig. 8. Time evolution of the hydroxyl concentration at various altitudes, which was retrieved using *a priori* information. The dash-dotted line shows the "true" dynamics of this component, the dotted line with markers denotes $\langle \mathrm{OH} \rangle_{\mathrm{med}}$, and the solid lines with markers indicate the boundaries of the interval $\langle \mathrm{OH} \rangle_{\mathrm{med}} \pm \sigma$.

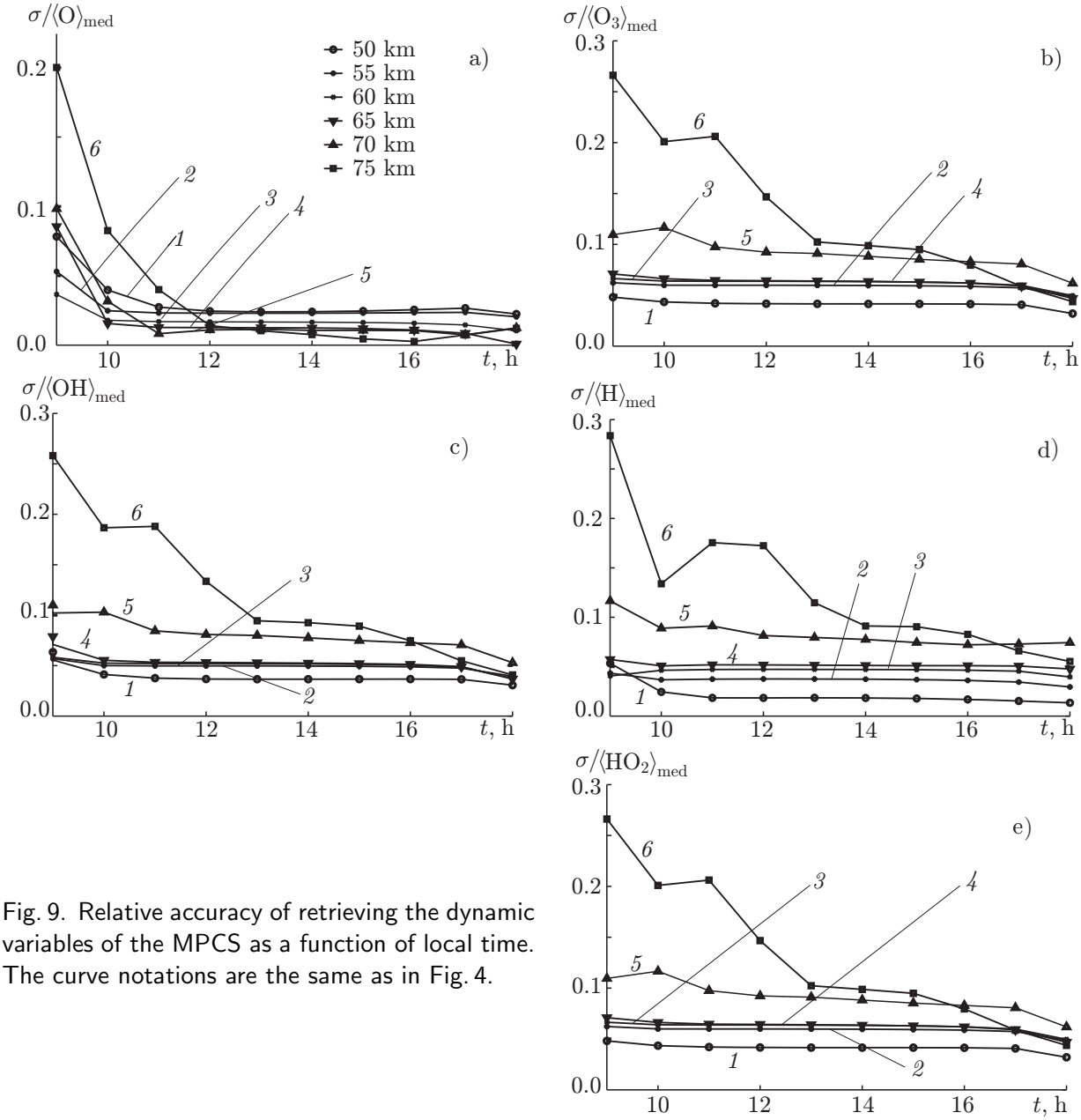

Fig. 9. Relative accuracy of retrieving the dynamic variables of the MPCS as a function of local time. The curve notations are the same as in Fig. 4.

H_2O concentration with the direct-measurement results. Second, the method allows us to obtain a very high accuracy of retrieving the concentrations of atomic oxygen and hydrogen, hydroxyl, and hydrogen peroxide. We recall that these components at the mesospheric altitudes cannot be measured from the Earth's surface, while the satellite-born devices are at present capable of measuring only hydroxyl. Third, the proposed method actually allows one to filter the noise of the microwave measurements of the ozone concentration at the mesospheric altitudes. Fourth, the processing of the long (many-day) ozone-concentration series on the assumption of invariability of the water-vapor concentration profile during each 24-h period makes it possible to retrieve slow spatiotemporal evolution of the water-vapor concentration.

A unique spectroradiometer–mobile ozonometer with the digital spectrum analyzer has recently been developed at the Institute of Applied Physics of the Russian Academy of Sciences [17]. The current basic characteristics of this device are as follows: the center frequency is 110.83604 GHz, the analysis bandwidth is 1 GHz, the spectral resolution is 61 kHz, the number of spectral channels is 16384, the total weight is about 15 kg, the typical time of accumulation of one spectrum, which is then used for retrieving one

ozone-concentration profile, amounts to about 15–30 min, and the total power consumption does not exceed 100 W. It has been elaborated to the expeditionary-level, totally automated device with a unique system of calibration of the measured signal against an internal electrically controlled standard. At present, we attempt to significantly reduce the integral noise temperature mainly due to using a new antenna system in the form of a conical corrugated horn with a low level of the side lobes and a pre-amplifier on the basis of the HEMT microchip. It is expected that this device will allow one to retrieve the vertical ozone-concentration profiles with accuracies no worse than those ensured by the OZORAM device. In what follows, to improve the quality of retrieval of the trace-gas concentrations, we plan to consider the described method within the framework of one statistical procedure and analyze the problem of obtaining the ozone-concentration profiles from the radiometric data when the spectra of the natural atmospheric radiation directly serve as the input experimental information.

This work was supported by the Russian Science Foundation (contract No. 15–17–10024 of June 04, 2015).

REFERENCES

1. F. J. Schmidlin, *Geophys. Res. Lett.*, **19**, No. 16, 1643 (1992).
2. http://andromeda.caf.dlr.de/ndmc .
3. G. P. Brasseur and S. Solomon, *Aeronomy of the Middle Atmosphere*, D. Reidel, Dordrecht (1‘986).
4. B. J. Sandor and R. T. Clancy, *J. Geophys. Res. D*, **103**, No. D11, 13337 (1998).
5. H. Takahashi, S. M. L. Melo, B. R. Clemesha, et al., *J. Geophys. Res. D*, **101**, No. D14, 4033 (1996).
6. J. Gumbel, D. P. Murtagh, P. J. Espy, et al., *J. Geophys. Res. A*, **103**, No. A10, 23399 (1998).
7. K. W. Jucks, D. G. Johnson, K. V. Chance, et al., *Geoph. Res. Lett.*, **25**, No. 2, 3935 (1998).
8. K. U. Grossmann, D. Offermann, O. Gusev, et al., *J. Geophys. Res.*, **107**, No. D23, 8173 (2002).
9. R. R. Conway, M. E. Summers, M. H. Stevens, et al., *Geophys. Res. Lett.*, **27**, No. 17, 2613 (2000).
10. http://mls.jpl.nasa.gov .
11. http://saber.gats-inc.com/index.php .
12. M. Yu. Kulikov, A. M. Feigin, and G. R. Sonnemann, *Radiophys. Quantum Electron.*, **49**, No. 9, 683 (2006).
13. M. Yu. Kulikov, A. M. Feigin, and G. R. Sonnemann, *Atmos. Chem. Phys.*, **9**, No. 21, 8199 (2009).
14. http://www.ndsc.ncep.noaa.gov .
15. S. V. Solomonov, K. P. Gaikovich, E. P. Kropotkina, et al., *Radiophys. Quantum Electron.*, **54**, No. 2, 102 (2011).
16. Yu. M. Timofeev, V. S. Kostsov, A. V. Poberovsky, et al., *St. Petersburg Univ. Bull., Ser. 4: Phys., Chem.*, No. 4, 44 (2008).
17. A. A. Krasil’nikov, M. Yu. Kulikov, L. M. Kukin, et al., *Radiophys. Quantum Electron.*, **56**, Nos. 8–9, 628 (2013).
18. M. Yu. Kulikov, A. A. Krasil’nikov, A. A. Shvetsov, et al., *Radiophys. Quantum Electron.*, **58**, No. 6, 409 (2015).
19. M. Yu. Kulikov, D. N. Mukhin, and A. M. Feigin, *Radiophys. Quantum Electron.*, **52**, No. 9, 618 (2009).
20. G. Sonnemann, C. Kremp, A. Ebel, and U. Berger, *Atmos. Env.*, **32**, No. 18, 3157 (1998).
21. M. Palm, C. G. Hoffmann, S. H. W. Golchert, et al., *Atmos. Meas. Tech.*, **3**, No. 6, 1533 (2010).

22. S. Studer, K. Hocke, A. Schanz, et al., *Atmos. Chem. Phys.*, **14**, No. 12, 5905 (2014).

23. A. Tarantola, *Inverse Problem Theory: Methods for Data Fitting and Model Parameter Estimation*, Elsevier, Amsterdam (1987).

24. http://www.ndsc.ncep.noaa.gov .